Article

J. Mex. Chem. Soc. **2007**, *51(3)*, 154-159

ISSN 1870-249X

Mesoporous Silica-Lanthanum: Characterization and Catalytic Activity on NO Reduction

Lourdes Díaz-Jiménez

Cinvestav-Saltillo, km 13.5 carretera Saltillo-Monterrey, 25900 Ramos Arizpe, Coahuila, México.
Tel: +52(844) 438-9612 Fax: +52(844) 438-9610 lourdes.diaz@cinvestav.edu.mx

Recibido el 1 de junio de 2007; aceptado el 26 de noviembre de 2007

Abstract. A series of ordered mesoporous silica-lanthanum materials was prepared. The influence of lanthanum into a silica matrix on the structural, textural and acidic properties is described. The mechanical and hydrothermal stability of mesoporous materials were evaluated. The catalytic activity of cobalt catalyst for selective reduction of nitrogen oxide -in the presence of propane- at temperatures between 350 and 550 °C, was tested. A selective reduction of NO by cobalt-based catalyst raised 18 %, at 450 °C.
Key words: SCR-NO, Co catalyst, mesoporous materials.

Resumen. Se preparó una serie de materiales mesoporosos de sílice-lantano. Se describe la influencia de la adición de lantano en las propiedades texturales, estructurales y ácidas. También se evaluó la estabilidad térmica e hidrotermal de los materiales. Se probó la actividad catalítica de cobalto, sobre uno de los materiales preparados, en la reducción selectiva de monóxido de nitrógeno con propano a temperaturas entre 350 y 550 °C. Se alcanzó una conversión de 18 % de NO a 450 ºC con el catalizador probado.
Palabras clave: Reducción selectiva de NO, catalizador de cobalto, materiales mesoporosos.

Introduction

The atmospheric pollution caused by continuous emission of the contaminants NOx and SOx has attracted importance around the world [1-3] because these are the major gases in global heating. Nitrogen oxides are produced in high concentrations during the combustion process in automotors and power plants. Decomposition of NO to N_2 and O_2 over a solid catalyst is a promising reaction for removing this pollutant from exhaust emissions [1, 4]. The selective catalytic reduction (SCR) of NO in the presence of ammonia has been the commercial process for NOx emission control from stationary resources. However, the use of ammonia involves many troubles, such as equipment corrosion and hazardous handle. For this reason, hydrocarbons have been preferred instead of ammonia for reducing NOx [5, 6]. In this sense, the Cu-ZSM5 catalyst has been successfully used for the NO selective catalytic reduction by hydrocarbons [7-9]. However, the oxygen present in the feed causes a partial oxidation of the catalyst surface decreasing its activity. Consecuently, zeolites containing a transition metal ion (i.e. Fe and Co) have been tested for selective catalytic reduction of NO and N_2O [10, 11].

In another hand, ordered mesoporous silica discovered by Mobil Oil Co. [12, 13] became one of the most important success in materials field at beginning of the 90'. Since then, many efforts have been devoted to the synthesis of analogous of that mesoporous silica, as potential catalysis for a number of applications [14-17]. The increasing interest on these mesoporous solids arises from many reasons, mainly from the existence of interesting properties such as their extremely high specific surface areas (> 1000 $m^2\ g^{-1}$) and their uniform porous network which diameters can be tuned between 15 and more than 100 Å. Furthermore, the synthesis of these materials can be afforded through a new and versatile approach based in a sol-gel methodology, where self-assembled aggregates of surfactant species seem to play a structure-directing role. In addition the disordered character of their inorganic wall can easily accommodate larger ions such as Al(III) [18], Cr(III) [19], Mn(II)[20], Fe(III) [21], Zr(IV) [22], which can replace to the Si(IV) species in tetrahedral positions. However, to the best of our knowledge, only a brief study has been undertaken concerning on the introduction of rare earth elements into a mesoporous silica matrix [23, 24].

It must be taken into account that lanthanum oxide has found applications in environmental and catalysis fields, since it is an important component of automobile exhaust-gas conversion catalysts, as a support for catalysts, and as a catalyst for oxidative coupling of methane [25-27]. Besides La_2O_3 is a basic metal oxide, and therefore the preparation of high surface area lanthanum-dopped silica can lead to suitable support to attain an excellent dispersion of active species –such as cupper or cobalt oxides- for the reduction of NOx.

Thus, the aim of this paper is to report the synthesis of ordered mesoporous silica-lanthanum materials (MSL) describing the influence of the incorporation of lanthanum into a silica matrix on the structural, textural and acidic properties of the resulting mesoporous materials, and on their mechanical and hydrothermal stability. In this sense, one MSL was used as support of cobalt oxides and tested for the selective catalytic reduction of NO using propane as reducing agent.

Results and discussion

Characterization of MSL materials

The powder X-ray diffraction (XRD) patterns of the MSL samples are shown in Figure 1. All of them show an intense

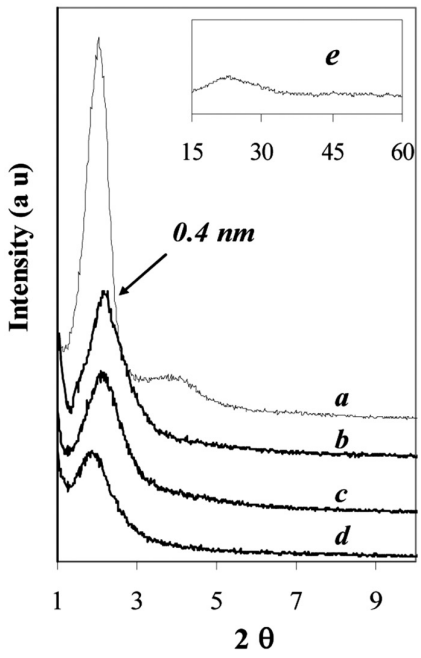

Fig 1. XRD patterns of (*a*) MS, (*b*) MSL50, (*c*) MSL25 and (*d*) MSL5, (*e*) MSL5 high 2θ angles.

low angle diffraction peak assigned to d_{100} reflection of a hexagonal structure, in agreement with materials of similar nature [13]. As reference, the XDR pattern of pure siliceous material (labeled MS) is included too. The incorporation of lanthanum into the silica matrix results in the increase the value of the d_{100} reflection from 3.4 to 4.7 nm. This modification might stem by the size of lanthanum ions are bigger that the silicon and occupies more space in the walls of the inorganic structure, besides tending to adopt a coordination over 4. Furthermore, as expected for larger rooms in inorganic walls, due to the presence of La(III) ions values of the wall thickness (Δ), became bigger in MSL's (see Table 1).

The absence of other diffraction peaks at higher angles, after calcinations of the MSL solids at 540 ºC (curve e, Fig. 1), is consistent with a lack of long-range hexagonal order or finite size effects. On the other hand, this fact discards the presence of extraframework lanthanum oxides. Thus, in order to be sure of the latter assumption, MSL5 was calcined in air at 800 ºC; its XRD pattern conserves the d_{100} diffraction peak and no signals corresponding to La_2O_3.

TG and chemical analyses confirmed that calcination at 540 ºC is effective for removing the organic matter, because the DTA curves show the absence of exothermic effect attributable to the organic matter; carbon and nitrogen percentages in calcined materials were always lower than 0.2 %. The TG analysis of the calcined samples provided, in turn, information of the hydrophilic nature of the pore network.

Textural parameters have been obtained from the nitrogen adsorption-desorption isotherms at 77 °K. The isotherms of the MSL samples are reversible and can be classified as Type IV in the IUPAC classification (Fig. 2) [28]. Table 1 exhibits the textural parameters obtained from the isotherms. The pore size distributions obtained by Cranston & Inkley method [29] reveals the formation of materials with a mesoporous structure. This distribution exhibits only a narrow peak with maximum radium between 1.0 to 1.5 nm (Fig. 2). The sample that presented a higher pore volume contains the lowest content of lanthanum, fact that is corroborated in the BET surface area (Table 1).

The surface area values for the MSL materials were relativity lower than the MS sample; these data are attributed to the increased mass of the MSL materials. The same effect was observed previously in mesoporous siliceous materials doped with aluminum, titanium, vanadium or zirconium [13-17].

The acidity properties of the calcined samples were determined by using temperature programmed desorption of ammonia (TPD-NH_3) and pyridine adsorption coupled to infrared spectroscopy (Table 3). The MSL TPD-NH_3 profiles have a small difference of MS sample. The later exhibits only a broad band of very low intensity, with a maximum centered at 430 ºC. It is assigned to strong Lewis acid sites, located probably on structural defects. In order to obtain a comparison among total acidity values, it is convenient to report them as acidity values per square meter of catalyst, taking into account the differences in the surface areas among all studied solids. Thus, an important increasing in the total acidity was observed when lanthanum was incorporated into the inorganic structure. The total desorbed amount of ammonia means that the acidity increased slightly with lanthanum insertion in the structure of

Table 1. Textural parameters and surface acidity of mesoporous silica-lanthanum materials.

Material	S_{BET} $m^2 g^{-1}$	V_p * $cm^3 g^{-1}$	d_p^a Å	ΔV_p^a $cm^3 g^{-1}$	thickness Å	TPD-NH_3 mmol NH_3 g^{-1}	Py adsorbed μmol g^{-1} C_L	C_B
MS	1135	0.98	27	1.17	18	0.66	14	4
MSL50	746	0.48	26	0.46	20	0.66	147	39
MSL25	577	0.39	26	0.39	22	0.70	150	62
MSL5	464	0.33	29	0.30	25	0.89	166	83

*P/P_0 = 0.95.

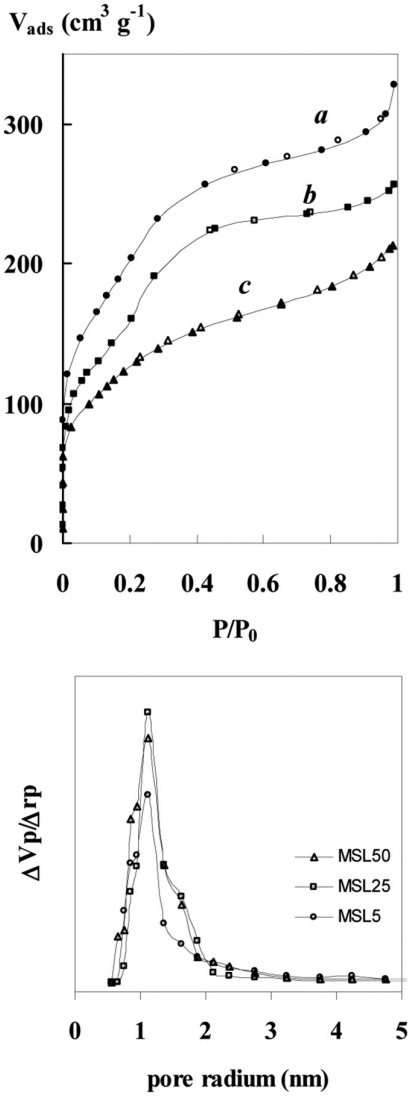

Fig. 2. N_2 (77 K) adsorption-desorption isotherms and pore size distribution of (*a*) MSL50, (*b*) MSL25 and (*c*) MSL5.

materials. The quantity of adsorbed pyridine provided information about the nature and concentration of the acid sites, this study are agreement with the TPD-NH_3 results; the major acidity is attributed to Lewis sites.

The mechanical and hydrothermal stability is an important parameter for any catalyst. Table 2 shows the principal textural parameters of MSL materials prior and after hydrothermal and mechanical tests. MS, MLS50 and MSL25 lost about 25 % surface area; but MS5 exhibited an important lost of specific surface area (33 %). However, all samples preserved the d_{100} diffraction peak. The pore size distribution didn't change visibly which could be closely related to a minimal pore thickness modification. That fact was previously observed in materials of same nature [21, 22].

Characterization of MSL catalysts

Table 3 summarizes the main physico-chemical properties of cobalt catalysts supported on MSL5 material. The porosity and crystallinity of support are preserved after impregnation or ion exchange processes. The XRD patterns of MSL5-Co, MSL5E-Co and support are similar; no evidence for Co_3O_4 species was present. The surface area diminishes after the processes of impregnation or ionic exchange with cobalt. The total acidity —determined by the adsorption of ammonia— decreases in comparison with that non-impregnated sample. This behavior probably itself due to the occlusion on behalf of the pores of the material, caused by CoO species deposited on the surface.

The catalysts prepared by incipient wetness impregnation with cobalt(II) acetate were pale pink and after calcination became dark green. Figure 3 shows the diffuse reflectance UV-VIS spectra for cobalt catalysts. The MSL5-Co catalyst exhibits three maximums about 531, 597 and 630 nm assigned to the isolated tetrahedral Co^{2+} species which could be attributed to $^4A_2 \rightarrow {}^4T_1\,(^4P)$, $^4A_2 \rightarrow {}^4T_1\,(^4F)$, and $^4A_2 \rightarrow {}^4T_2$ transitions agreement with previous studies on cobalt catalyst supported on a Sib zeolite [30] and $CoAl_2O_4$ [31].

The spectrum of the MSL5E-Co catalyst presents similar features to MSL5-Co: three bands between 500 and 800 nm,

Table 2. Textural parameters of mesoporous silica-lanthanum materials after mechanical and hydrothermal tests.

Material	Parameter	Raw material	After mechanical test	After hydrothermal test
MS	S_{BET} ($m^2 g^{-1}$)	1135	867	925
	V_p ($cm^3 g^{-1}$)	0.98	0.56	0.57
	d_{100} (nm)	3.88	3.79	3.92
MSL50	S_{BET} ($m^2 g^{-1}$)	746	554	591
	V_p ($cm^3 g^{-1}$)	0.48	0.45	0.37
	d_{100} (nm)	4.03	3.98	—
MSL25	S_{BET} ($m^2 g^{-1}$)	577	447	453
	V_p ($cm^3 g^{-1}$)	0.39	0.28	0.30
	d_{100} (nm)	4.12	4.07	4.09
MSL5	S_{BET} ($m^2 g^{-1}$)	464	312	325
	V_p ($cm^3 g^{-1}$)	0.33	0.22	0.24
	d_{100} (nm)	4.69	4.42	4.48

Table 3. Textural parameters of cobalt catalysts.

Catalyst	S_{BET} ($m^2 g^{-1}$)	Total acidity (mmol NH_3 g^{-1})	UV-VIS-NIR DRS (nm)
MSL5-Co	152	0.57	531, 597, 630, 1360, 1540
MSL5E-Co	292	0.64	330, 505, 630, 1325, 1440
MSL5	464	0.89	—

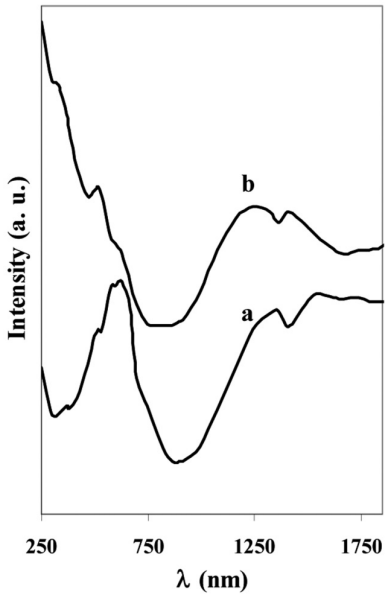

Fig. 3. DR UV-vis spectra of (a) MSL5-Co and (b) MSL5E-Co catalysts.

and two broad bands at 1360 and 1540 nm. Moreover, according to the previous data reported for a cobalt alumina pillared zirconium phosphate catalyst [32], the presence of a broad band about 500 nm evidences the existence of CoO_x oligomers, probably formed on the support during the calcination process. The presence of CoO_x species were suggested before as argument to explain the surface area and total acidity diminishing.

The temperature-programed reduction profiles of cobalt catalyst by hydrogen are shown in Figure 4. Both catalysts exhibit a broad peak at temperatures higher than 550 °C; in both cases a shoulder between 750 and 800 °C was observed. This peak at 550 °C could be assigned to the Co^0 reduced species, just as it was stated for a cobalt-based alumina pillared zirconium phosphate [33]. The shoulder is explained by the existence of Co^{2+} species created by the structural nearness of lanthanum and silicon ions, or by the dispersed CoO units or by the formation of cobalt spinel with lanthanum in the internal surface of the support by diffusion of Co^{2+} ions during calcination. In another hand, it is noticeable the presence of a small peak between 275 and 350 °C for the MSL5-E-Co catalyst. This could be assigned to the presence of Co^{3+} species formed during the calcination process of the catalyst.

Figure 5 shows the temperature-programmed desorption profiles of pre-adsorbed NO at room temperature on two different cobalt catalysts: (a) MSL5E-Co and (b) MSL5-Co. On MSL5E-Co catalyst, two desorption peaks of NO were observed, one intense peak appear at 195°C and a second one, broader, at 350 °C, whereas for MSL5-Co catalyst, only one broad desorption signal at 253 °C was observed. The TPD of NO profile on MSL5E-Co is agreement with a previously reported catalyst [34]. The first desorption peak observed on MSL5E-Co could be due to the cobalt species exchanged in the framework, and the second peak must be due to the NO

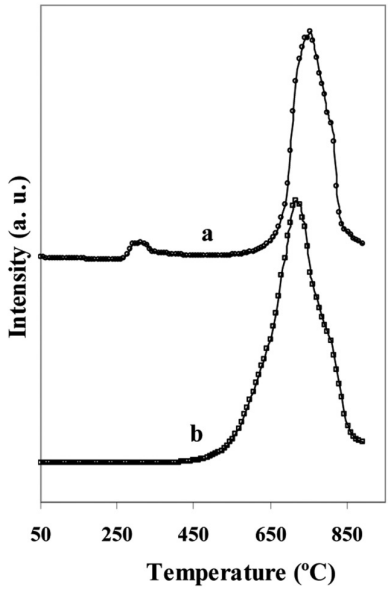

Fig. 4. H_2-TPR profiles of (a) MSL5-Co and (b) MSL5E-Co catalysts.

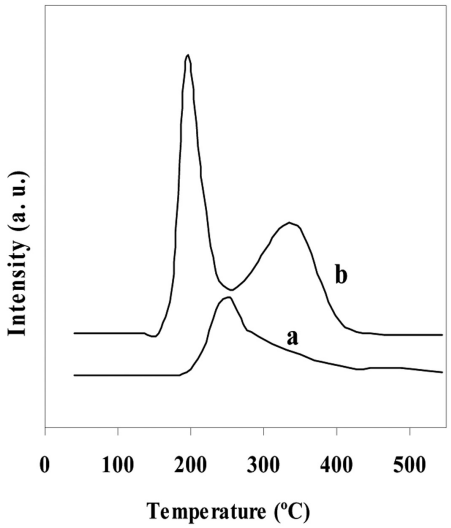

Fig. 5. NO-TPD plots of (a) MSL5E-Co and (b) MSL5-Co catalysts.

desorption by the Co deposited on the surface of the catalyst. This fact is in agreement with the only desorption peak observed for the MSL5-Co catalyst.

Catalytic results

The cobalt catalysts supported on MSL5 have been tested for selective reduction of NO using propane as reducing agent, in the presence of oxygen.

Figure 6 presents the results of the catalytic studies. For the MSL5E-Co catalyst the maximum conversion of NO was 18.3 %, reached at 450 °C, while MSL5-Co converted only 9.8 % of NO at the same temperature. This fact is could be due at the higher acidity of the MSL5E-Co catalyst, determined by NH_3-TPD, which lead to a total oxidation of reducing agent (see Table 3), as can be inferred from Figure 6b in which for the MSL5E-Co converted a 98 % of propane at 450 °C. The MSL5E-Co catalyst was more active than other cobalt catalysts. For CoO supported on alumina, methane was used as reducing agent; in this case no more than 10 % of NO conversion at 450 °C was observed, although this catalyst was slightly more active at higher temperatures [35]. In another hand for Co supported on alumina-zirconium phosphate, NO conversion was 14 %, using propane at 450 °C [33]. The MSL5E-Co catalytic activity suggests a good dispersion of the active phase (CoO) on the network of the MSL5 material.

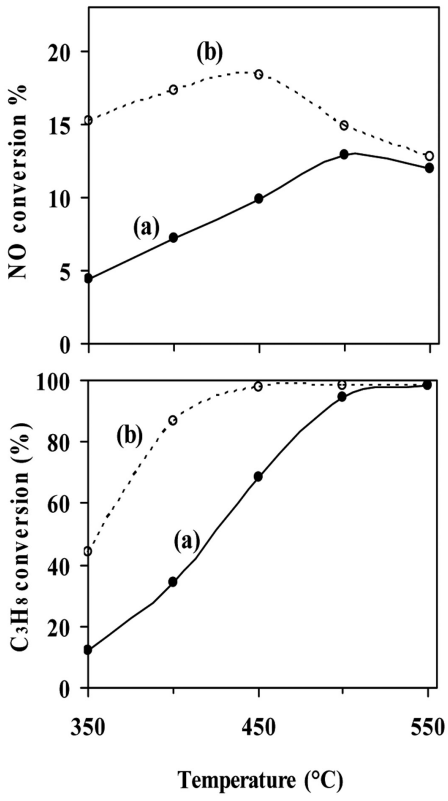

Fig. 6. Temperature reaction dependence of NO and propane conversion for (a) MSL5E-Co and (b) MSL5-Co catalysts.

Experimental

Synthesis

The lanthanum-doped silica solids with Si/La molar ratio of 5, 25 and 50 were prepared following a previously described method [36]. In brief, they were prepared by putting in contact, under vigorous stirring, a 25 wt% cetyltrimethylammonium bromide (CTMABr) aqueous solution, previously treated at 80 ºC for 30 min, with a lanthanum(III) acetate aqueous solution. This solution was added to an ethanolic solution of tetraethyl orthosilicate (TEOS), and the resulting gel was stirred at room temperature for 7 days. Then, solids were recovered by centrifugation, washed with ethanol and air dried at 60 ºC. Finally, these precursor solids were calcined in air at 550 ºC for 6 hours (1.5 ºC min^{-1} heating rate), in order to remove the organic moieties after exerting its structuring effect on the inorganic network. The resulting mesoporous materials were labeled as MSL*x*, where *x* denotes the Si/La molar ratio. A mesoporous silica (labeled MS) was also prepared.

The MSL5-Co catalysts was prepared using the incipient wetness method and by ion exchange. Thus, 1 g of MSL5 material was treated with a cobalt(II) acetate aqueous solution containing the amount of Co^{2+} to reach a 6 wt%. A cobalt exchanged catalyst (MSL5E-Co) was prepared with an aqueous solution of cobalt(II) acetate containing an amount corresponding to 10 times the cation exchange capacity of the support. After impregnation, both catalysts were firstly heated at 60 °C and then at 550 °C for 5 h in air (1 °C min^{-1} heating rate).

Characterization

Powder X-ray diffraction patterns were recorded on a Siemens D-501 diffractometer equipped with a graphite monochromator and using the Cu Kα radiation (λ = 154.05 pm).

Mechanical stability of the lanthanum-doped mesoporous silica has been evaluated by pressing the powdered samples at 5.7 kg cm^{-2} and conforming as pellets of sized comprised between 0.125 and 0.250 mm. On the other hand, the hydrothermal stability of the catalysts was studied by treating the samples at 550 ºC under a flow of nitrogen saturated with water vapor for 6 hours.

Textural parameters have been obtained from the nitrogen adsorption-desorption isotherms using a volumetric method in a glass conventional apparatus at –196 °C (samples were outgassed at 200 °C and 10^{-4} Pa overnight).

Diffuse reflectance UV–VIS spectroscopy analysis were carried out at room temperature using a Shimadzu MPC 3100 spectrometer. $BaSO_4$ was used as reference for the MSL*x* materials, while for the catalysts, MSL5 was used as reference. Pyridine adsorption coupled to IR spectroscopy was employed to determine the acidity of MSL*x* materials. For the adsorption of pyridine, self-supported wafers were placed in a vacuum cell assembled with Teflon stopcocks and CaF_2 win-

dows. IR spectra were recorded on a Perkin-Elmer 810 spectrometer. The samples were evacuated (350 °C, 10^{-2} Pa overnight), exposed to pyridine vapors at room temperature, and then outgassed between room temperature and 300 °C.

The concentration of acid sites was estimated for the integrated absorption at 1550 and 1450 cm^{-1}, using the extinction coefficients: EB = 0.73 cm · μmol^{-1} and EL = 1.11 cm · μmol^{-1} for Brønsted and Lewis sites, respectively [37]. Temperature-programmed reduction (TPR) experiments of catalysts were performed between 100 and 700 °C, using a flow of Ar/H_2 (40 ml min^{-1}, 10 % of H_2) and a heating rate of 10 °C min^{-1}. Water produced in the reduction reaction was eliminated by passing the gas flow through a cold finger (–80 °C). The consumption of hydrogen was controlled by an on-line gas chromatograph provided with a TCD.

For NO-TPD assays, the catalyst were first treated with a NO flow for 1 h at room temperature (150 cm^3 min^{-1} flow rate and 0.05 vol% NO balanced with He). Later, the catalyst was desorpted using a heating rate of 10 °C min^{-1} between 40 and 550 °C. Previously to the NO adsorption, the catalysts were heated at 500 °C under He flow for 1 h. During desorption, the composition of gases were continuously monitored by using an on-line quadrupole mass spectrometer (Balzers GSB 300-02).

Catalytic test:

The activity of catalysts in the SCR of NO by propane was measured in a flow microreactor (Pyrex glass tube, 0.27 in o.d.) coupled to a mass spectrometer (Balzers GSB 300-02). Approximately 150 mg of catalysts pellets (0.3-0.4 mm) were packed into the reactor and plugged with glass wool. Before the tests, the catalysts were heated up in situ at 500 °C for 30 min under helium flow. The reaction mixture consisted of 1000 ppm NO, 1000 ppm propane and 2.5 vol% O_2. The flows were independently controlled by channel mass flowmeters and a total flow rate of 150 cm^3min^{-1} was used in the feed. Under these experimental conditions, the space velocity was 60000 $cm^3h^{-1}g^{-1}$. In standard conditions, the interval of temperature explored was 350-550 °C. The concentration of NO and propane as other gaseous products were monitored using an on line quadrupole mass spectrometer (Balzers GSB 300-02).

Acknowledgements

The author acknowledges to Departamento de Química Inorgánica, Cristalografía y Mineralogía, of Málaga University (Spain) for the support on experimental. Also thanks to CONACYT for a fellowship number 93793.

References

1. Li, G.; Larsen, S.C.; Grassian; V.H. *J. Molec. Catal. A Chemical* **2005**, 227 (1), 25.
2. Delahay, G.; Coq, B. *Catal. Sci. Ser*. **2002**, 3, 345.
3. V.H. Grassian *Int. Rev. Phys. Chem.* **2001**, 20, 467.
4. Ruckenstein, E.; Hu, Y.-H. *Ind. Eng. Chem. Res*. **1997**, 36, 2533.
5. Zhang, R.D.; Villanueva, A.; Alamdari, H.; Kaliaguine, S. *Appl. Catal. A* **2006**, 207, 85.
6. Zhang, R.D.; Villanueva, A.; Alamdari, H.; Kaliaguine, S. *Appl. Catal. B* **2006**, 64, 220-233.
7. Iwamoto, M.; Hamada, H. *Catal. Today* **1991**, *10*, 57.
8. Zhang, W.X.; Yahiro, H.; Mizuno, N.; Izumi, J.; Iwamoto, M. *Langmuir* **1993**, *9*, 2337.
9. Sjöval, H.; Olsson, L.; Fridell, E.; Blint, R.J. *Appl. Catal. B* **2006**, *64*, 180.
10. Li, Y.J.; Armor, J.N. *Appl. Catal. B* **1992**, *1*, L31.
11. Li, Y.J.; Slager, T.L.; Armor, J.N. *J. Catal*. **1994**, *150*, 388.
12. Beck, J.S. US Patent 5057296, **1991.**
13. Beck, J.S.; Vartulli, J.C.; Roth, W.J.; Leonowicz, M.E.; Kressge, C.T.; Schmitt, K.D.; Chu, C.T.W.; Olsen, D.H.; Sheppard, E.W.; McCullen, S.B.; Higgins, J.B.; Schlenker, J.L. *J. Am. Chem. Soc*. **1992**, *114*, 10834.
14. Luan, Z.; Cheng, C.-F.; Zhou, W. ; Klinowski, J. *J. Phys. Chem*. **1995**, *99*, 1018.
15. Tanev, P.T.; Chibwe, M.; Pinnavaia, T.J. *Nature* **1994**, *368*, 321.
16. Jones, D.J.; Jimenez-Jimenez, J.; Jimenez-Lopez, A.; Maireles-Torres, P.; Olivera-Pastor, P.; Rodriguez-Castellon, E.; Roziere, E. J., *J. Chem. Soc., Chem. Commun*. **1997**, 431.
17. Cheng, S.; Das, D. US Patent 6497857, **2002**.
18. Tuel, A.; Gontier, S.; Teissier, R. *J. Chem Soc. Chem. Commun*. **1996**, 651.
19. Zhang, W.; Pinnavaia, T.J., *Catal. Lett*. **1996**, *38*, 261.
20. Zhang, W.; Wang, J.; Tanev, P.T.; Pinnavaia, T.J. *J. Chem Soc. Chem. Commun.* **1996**, 979.
21. He, N.Y., Bao, S.L., Xu, Q.H. *Stud. Surf. Sci. Catal.* **1997**, *105*, 85.
22. Jones, D.J.; Jiménez-Jiménez, J.; Jiménez-López, A.; Maireles-Torres, P.; Olivera-Pastor, P.; Rodríguez-Castellón, E.; Rozière, J. *J. Chem. Soc,.Chem. Commun*. **1997**, 431.
23. Kloetstra, K. R.; Vanderbroek, J.; Vanbekkum, H. *Catal. Lett.* **1997**, *47*, 235.
24. Chen, C.-Y.; Li, H.-H.; Davis, M. E. *Microporous Mat.* **1993**, *2*, 17.
25. Fokema, M.D. ; Ying, J.Y. *Appl. Catal. B* **1998**, *18*, 71.
26. Petryk, J.; Kolakowska, E. *Appl. Catal. B* **2000**, *24*, 121.
27. Mescia, D.; Cauda, E.; Russo, N.; Fino, D.; Saracco, G.; Specchia, V. *Catal. Today* **2006**, *117*, 369.
28. Sing, K.S.W; Everett, D. H.; Haul, R.A.W.; Moscou, L.; Pierotti, R.A.; Rouquerol, J.; Siemieniewska, T. *Pure Appl. Chem.* **1985**, *57*, 603.
29. Cranston, R.W.; Inkley, F.A. *Adv. Catal*. **1957**, *9*, 143.
30. Dzwigaj, S.; Janas, J.; Machej, T.; Che, M. *Catal. Today*. **2007**, *119*, 133.
31. Yan, J.; Kung, M.C.; Sachtler, W.M.H.; Kung, H.H. *J. Catal*. **1997**, *172*, 178.
32. Fierro, G.; Eberhardt, M.A.; Houalla, M.; Hercules, D.M; Hall, W.K. *J. Phys. Chem*. **1996**, *100*, 8468.
33. Hernández-Huesca, R.; Braos-García, P.; Mérida-Robles, J.; Maireles-Torres, P.; Rodríguez-Castellón, E.; Jiménez-López, A. *Chemosphere* **2002**, *48*, 467.
34. Marques, R.; El Kabouss, K.; Da Costa, P.; Da Costa, S.; Delacroix, F.; Djéga-Mariadassou, G. *Catal. Today* **2007**, *119*, 166.
35. Yan, J.Y.; Saxhtler H.H.; Kung, W.M.H. *J. Catal*. **1998**, *175*, 294. 32.
36. Jiménez-López, A.; Rodríguez-Castellón, E.; Maireles-Torres, P.; Díaz, L.; Mérida-Robles, *J. Appl. Catal. A* **2001**, 218, 295.
37. Datka, J.; Turek, A.M.; Jehng, J.M.; Wachs, I. E., *J. Catal*. **1992**, 135, 186.